

This article was downloaded by:

On: 25 January 2011

Access details: *Access Details: Free Access*

Publisher *Taylor & Francis*

Informa Ltd Registered in England and Wales Registered Number: 1072954 Registered office: Mortimer House, 37-41 Mortimer Street, London W1T 3JH, UK



Separation Science and Technology

Publication details, including instructions for authors and subscription information:

<http://www.informaworld.com/smpp/title~content=t713708471>

Study of Asymmetric Polarization in Direct Contact Membrane Distillation

M. Khayet^a; M. P. Godino^a; J. I. Mengual^a

^a Department of Applied Physics I, University Complutense of Madrid, Madrid, Spain

Online publication date: 08 July 2010

To cite this Article Khayet, M. , Godino, M. P. and Mengual, J. I.(2005) 'Study of Asymmetric Polarization in Direct Contact Membrane Distillation', *Separation Science and Technology*, 39: 1, 125 — 147

To link to this Article: DOI: 10.1081/SS-120027405

URL: <http://dx.doi.org/10.1081/SS-120027405>

PLEASE SCROLL DOWN FOR ARTICLE

Full terms and conditions of use: <http://www.informaworld.com/terms-and-conditions-of-access.pdf>

This article may be used for research, teaching and private study purposes. Any substantial or systematic reproduction, re-distribution, re-selling, loan or sub-licensing, systematic supply or distribution in any form to anyone is expressly forbidden.

The publisher does not give any warranty express or implied or make any representation that the contents will be complete or accurate or up to date. The accuracy of any instructions, formulae and drug doses should be independently verified with primary sources. The publisher shall not be liable for any loss, actions, claims, proceedings, demand or costs or damages whatsoever or howsoever caused arising directly or indirectly in connection with or arising out of the use of this material.

Study of Asymmetric Polarization in Direct Contact Membrane Distillation

M. Khayet,* M. P. Godino, and J. I. Mengual

Department of Applied Physics I, University Complutense of Madrid,
Madrid, Spain

ABSTRACT

The objective of this study was to analyze the polarization phenomena in each side of a microporous hydrophobic membrane using a direct contact membrane distillation process. Experiments were conducted with distilled water and sodium chloride aqueous solutions as feeds. Different flow rates and temperatures at both membrane sides were employed. The feed and permeate temperature polarization coefficients as well as the feed and permeate vapor pressure polarization coefficients were defined and evaluated. Two methods: a velocity extrapolation method and a semiempirical method that considers the heat and mass transfer empirical correlations, were used. It was proved that there is an asymmetric polarization in direct contact membrane distillation.

*Correspondence: M. Khayet, Department of Applied Physics I, University Complutense of Madrid, Avda Complutense s/n, 28040 Madrid, Spain; Fax: +34-91-3945191; E-mail: khayetm@fis.ucm.es.

Key Words: Membrane distillation; Vapor pressure polarization; Temperature polarization; Concentration polarization; Heat and mass transfer.

INTRODUCTION

Direct contact membrane distillation (DCMD) is a membrane distillation (MD) configuration in which a hydrophobic microporous membrane separates two aqueous solutions with different temperatures and composition. The presence of only a vapor phase inside the membrane pores is a necessary condition for MD to be carried out. In fact, the hydrophobic nature of the membrane prevents the penetration of liquid solution into the pores unless a hydrostatic pressure difference exceeding the liquid entry pressure of water (LEP_w) is applied.^[1] If this condition is fulfilled, liquid–vapor interfaces are formed at both pore sides. Consequently, a transmembrane temperature difference induces a water vapor pressure difference, which is the driving force in MD. As a result, water molecules evaporate at the hot interface, cross the membrane pores in vapor phase, and condense in the cold membrane interface side. Thus, MD separation is based on the liquid–vapor equilibrium state of the solution corresponding to the temperature at the membrane surface and the pressure within the membrane pores. In MD, nearly 100% of nonvolatile constituents are rejected and the process can be performed at a feed temperature considerably lower than the boiling point.

It is well known that transmembrane water flux leads to the appearance of the polarization phenomenon of the driving force by means of the temperature and concentration polarization at the membrane surfaces, as the vapor pressure depends on temperature and concentration. In fact, as can be observed in Fig. 1 when nonvolatile solutes are present in the feed side, the temperature in the bulk phases are different from the corresponding temperature on the membrane surfaces and the concentration is higher at the membrane surface than in the bulk phase.

A large number of studies have been undertaken to analyze the influence of temperature polarization on MD performance.^[2–6] In each of these studies, the investigators showed that this phenomenon has a significant effect on MD flux. Low feed and permeate circulation velocities, which result in low Reynolds numbers, can reduce the MD flux by orders of magnitude relative to high velocities, which induce large Reynolds numbers.

The temperature polarization coefficient is usually estimated assuming that its value is the same at both membrane sides.^[1–5] This means an assumption of equal feed and permeate heat-transfer coefficients. However, the heat-transfer coefficients at each side of the membrane are expected to be



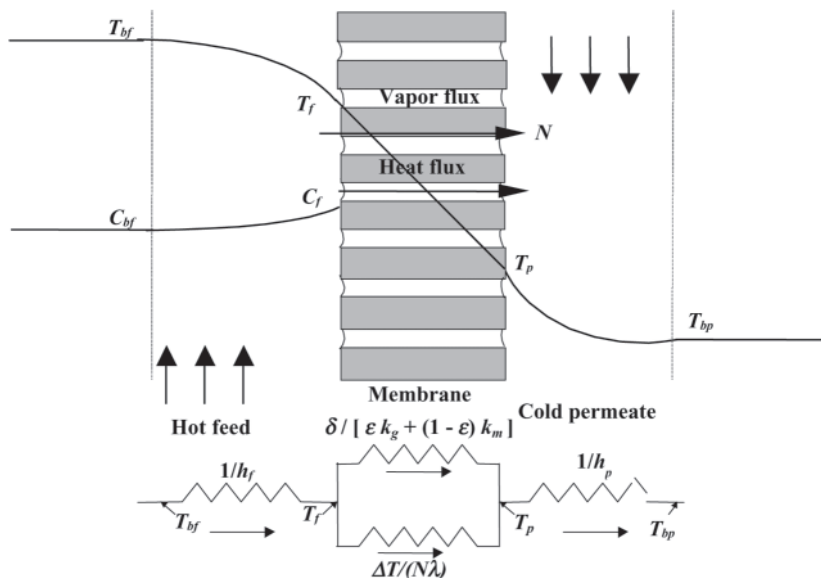


Figure 1. Concentration and temperature profiles in direct contact membrane distillation.

different as the temperature, type of solutions (i.e., density, viscosity, thermal conductivity, heat capacity, etc.), and, generally, the hydrodynamic conditions are different. As a consequence, the polarization coefficient of each phase adjoining the membrane must be different and subsequently, the mean temperature may be different from the one calculated between the bulk phases. This results in an asymmetric temperature profile, or which is the same an asymmetric vapor pressure profile through the composite system "hot boundary layer-membrane-cold boundary layer." Moreover, one of the methods used to determine the temperature polarization coefficient is Schofield's model.^[2] This model is based on the assumption of the linearization of the exponential dependence of the vapor pressure with temperature. This fact is valid only when water or diluted solutions are used and for small temperature differences between the feed and permeate.^[2] Consequently, the associated assumptions can result in large errors if they are applied to a realistic MD system.

In MD, there is a simultaneous presence of temperature and concentration polarization. Similarly to what occurs to the temperature, the concentration cannot be directly measured at the membrane surfaces but may only be obtained using some approximations. The Nernst film model, which neglects the eddy



and thermal diffusions in relation to the ordinary diffusion, is frequently used in MD.^[1,3] The use of mass transfer empirical correlations is necessary to determine the involved mass-transfer coefficient. In general, in DCMD systems, the quantitative effect of the concentration polarization is usually chosen to be negligible as compared with that of temperature polarization.^[3,5]

Because the driving force in MD is the vapor pressure difference, it is convenient to use the vapor pressure polarization coefficient. This coefficient represents the fraction of the externally applied driving force that contributes to the mass transfer and is essentially affected by changes in both temperature and composition.

In this study, an attempt was made to evaluate the temperature polarization coefficients and the vapor pressure polarization coefficients on each side of the membrane (i.e., in the feed side and in the permeate side) as well as the overall polarization coefficients. A velocity extrapolation method and a semiempirical method were used. DCMD was studied experimentally in a shell-and-tube capillary membrane module using distilled water and aqueous solutions of NaCl as feed. Different experimental conditions referring to temperature and circulation velocity of the feed in the lumen and permeate in the shell side were considered.

EXPERIMENTAL

The experimental system used to conduct the DCMD tests is shown in Fig. 2. A commercial shell-and-tube capillary membrane module MD020CP2N, supplied by Mycrodyn (Modulbau GmbH & Co. Kg, Germany) was used. Basically, it consists of a set of equal polypropylene porous hydrophobic capillaries. Its principal characteristics, as specified by the manufacturer, are as follows: number of capillaries: 40; membrane pore size: 0.2 μm ; inner capillary diameter: 1.8 mm; outer capillary diameter: 2.6 mm; effective filtration area of the membrane: 0.1 m^2 ; LEP_w : 140 kPa; fractional void volume: 70%; length of capillaries: 470 mm.

Distilled water and NaCl aqueous solutions were employed in the experiments. The solute concentration in the feed and in the permeate was measured continuously, in steady state, with a conductivimeter 712 Ω Metrohm. The hot feed solution was circulated in the lumen side of the membrane module and its shell side was circulated by cold distilled water.

The temperatures of the hot feed and cold permeate were measured at the inlets and at the outlets of the membrane module with Pt100 probes connected to a digital multimeter Keithley 199, with an accuracy of $\pm 0.1^\circ\text{C}$. The feed temperature was controlled by a thermostat Lauda K20KS connected to a heat exchanger located between the pump and the membrane module, whereas the



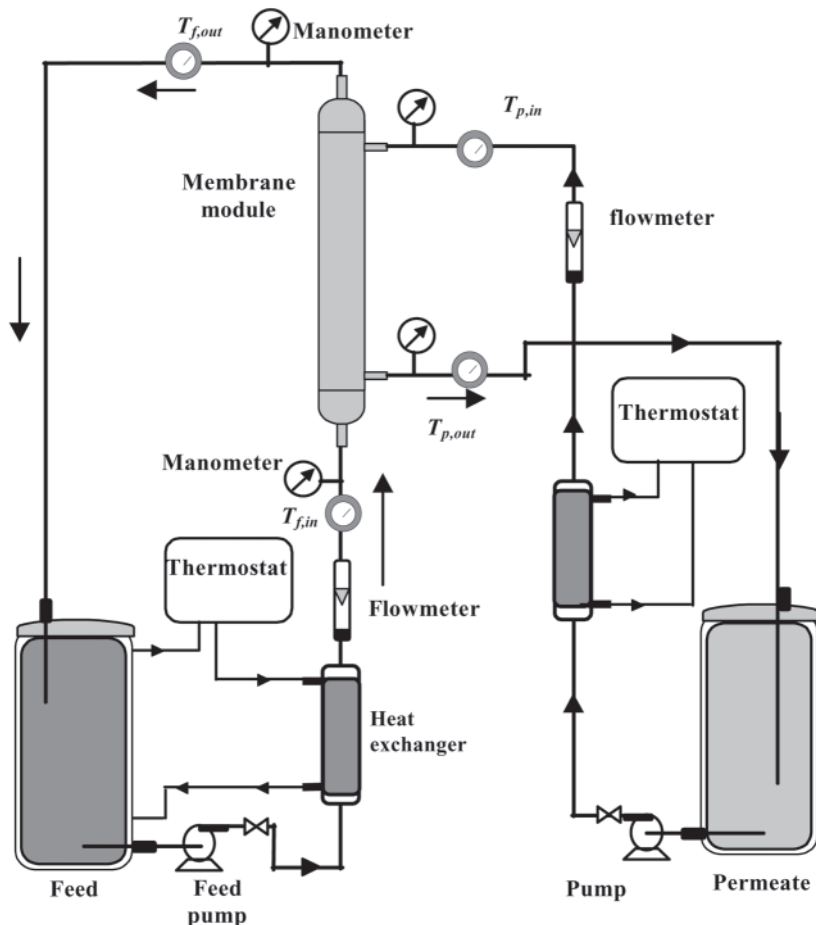


Figure 2. Experimental device.

permeate temperature was controlled by a refrigerated recirculator Poly-Science Model 675. The whole system was entirely insulated to minimize heat loss to the surroundings.

The hot and cold solutions were circulated with circulation pumps March TE-5.5C.MD and the flow rates were measured with flowmeters Tecfluid TCP 316-0630, with a precision of $\pm 2\%$.

The pressure difference through the membrane was controlled continuously with four manometers placed in the feed and permeate sides, at the inlets and outlets of the membrane module.



When using distilled water as feed, the MD flux was calculated by measuring the volume of the feed and permeate, with the help of graduated tubes connected to each container, during at least 3 hours and adjusting the experimental pairs of data (volume–time) to a straight line by the least squares method. The correlation coefficient was always better than 0.999, which means that the procedure is adequate. The total volume of water lost in the feed container was compared to the volume of permeate collected at the end of each experimental run. The agreement was good (4% in the worst case). In fact, these procedures permit the detection of any membrane wetting as well as any water evaporation from the feed container. When using salt aqueous solutions, the concentration in the feed container was maintained constant in each experimental test.

THEORY

In DCMD, the permeated flux is driven by a transmembrane vapor pressure difference, resulting from the imposed temperature difference (see Fig. 1). In our previous work,^[6] theoretical models were proposed to analyze the physical nature of the transmembrane flux through various types of microporous and hydrophobic membranes in DCMD configuration. The comparison between the theoretical predictions and the experimental results revealed that the combined Knudsen-molecular diffusive flux is responsible for the transport and the net MD coefficient, B , was written:

$$B = \frac{N}{\Delta P_v} = \frac{M}{RT} \left(\frac{1}{D_k} + \frac{P_a}{D_d} \right)^{-1} \frac{1}{\delta} \quad (1)$$

In this equation, N is the MD flux, ΔP_v is the transmembrane vapor pressure difference, δ is the membrane thickness, M is the water molecular mass, R is the gas constant, P_a is the air pressure, and the remaining coefficients are given by:

$$D_k = \frac{2\epsilon r}{3\tau} \left(\frac{8RT}{\pi M} \right)^{1/2} \quad (2)$$

$$D_d = \frac{\epsilon}{\tau} P D \quad (3)$$

where r is the membrane pore size, ϵ is the fractional void volume of the membrane, τ is the pore tortuosity, P is the total pressure, and D is the water diffusion coefficient.

Due to the presence of boundary layers adjoining both faces of the membrane, as observed in Fig. 1, there is a decrease of the driving force and



Eq. (1) cannot be used directly in its present form. In other words, the transmembrane pressure difference, ΔP_v , and the value corresponding to the bulk phases, ΔP_{vb} , are different. In this case, we introduce in Eq. (1) the vapor pressure polarization coefficient, η , which represents the fraction of the externally applied driving force that contributes to the mass transfer.

$$\eta = \frac{\Delta P_v}{\Delta P_{vb}} = \frac{B_b}{B} \quad (4)$$

where B_b is the global MD coefficient.

In MD, simultaneously to mass transport, heat transfer occurs across the membrane. Under steady-state conditions the heat transfer through the composite system “hot boundary layer-membrane-cold boundary layer” may be summarized in the following equation as stated in previous works:^[1,2,4]

$$h_f(T_{bf} - T_f) = N\lambda + \frac{\varepsilon k_g + (1 - \varepsilon)k_m}{\delta} (T_f - T_p) = h_p(T_p - T_{bp}) \quad (5)$$

where h_f and h_p are the heat-transfer coefficients established from the feed bulk solution to the membrane surface and from the permeate membrane surface to the permeate bulk solution, respectively; T_{bf} , T_f , T_p , and T_{bp} are the temperatures in the feed bulk solution, at the feed membrane surface, at the permeate membrane surface, and in the permeate bulk solution, respectively; λ is the latent heat of vaporization, and k_g and k_m are the thermal conductivities of the gas in the membrane pores and of the membrane matrix, respectively.

The derived Eq. (5) says that the amount of heat transferred from the feed side to the membrane surface is equal to the amount of heat transported inside the membrane and is equal to the amount of heat transferred to the permeate side (see Fig. 1). The heat transported through the membrane consists of the latent heat accompanying the vapor flux and the heat transferred by conduction across both the membrane material and the gas present in the membrane pores.

According to our previous work,^[7] the overall heat-transfer coefficient for the DCMD process may be written as:

$$H = \left[\frac{1}{h_f} + \frac{1}{\varepsilon k_g + ((1 - \varepsilon)/\delta) + k_m + (N\lambda/T_f - T_p)} + \frac{1}{h_p} \right]^{-1} \quad (6)$$

and the temperature polarization coefficient, θ , might be expressed as:

$$\theta = \frac{\Delta T}{\Delta T_b} = \frac{T_f - T_p}{T_{bf} - T_{bp}} = 1 - \frac{H}{h} \quad (7)$$



where h is the overall heat-transfer coefficient valid for the hot feed and cold permeate phases:

$$h = \frac{h_f h_p}{h_f + h_p} \quad (8)$$

Equations (7) and (8) may be rearranged as:

$$\theta = \theta_f + \theta_p - 1 \quad (9)$$

where θ_f and θ_p are the temperature polarization coefficients corresponding to the feed and permeate phases, respectively; and are defined in Eqs. (10) and (11) as follows.

$$\theta_f = 1 - \frac{H}{h_f} = \frac{T_f - T_{bp}}{T_{bf} - T_{bp}} \quad (10)$$

$$\theta_p = 1 - \frac{H}{h_p} = \frac{T_{bf} - T_p}{T_{bf} - T_{bp}} \quad (11)$$

The DCMD process is controlled by a mass transfer through the membrane and a heat transfer through the composite system formed by the membrane plus the adjoining layers. Both mechanisms are interrelated. In principle, four possibilities may occur:

1. If the heat transfers through the feed and permeate are very large, the temperatures at the membrane surfaces approach to the corresponding temperatures in the bulk phases. This means that the temperature polarization coefficients, θ_f and θ_p , [see Eqs. (10) and (11)], as well as the overall temperature polarization coefficient, θ , approach unity [see Eq. (9)].
2. If both the feed and permeate heat-transfer coefficients are small, the differences between the temperatures at the membrane surfaces and the temperatures corresponding to the bulk phases are high. This means that the temperature polarization coefficient, θ , approaches zero [see Eq. (7)]. In this case, the temperature polarization effects are very important and the heat-transfer resistances of the boundary layers control the DCMD process.
3. If the permeate heat-transfer coefficient is very large in comparison to the feed heat-transfer coefficient, the temperature at the permeate membrane surface is similar to the corresponding temperature at the bulk phase. This means that the permeate temperature polarization coefficient, θ_p , approaches unity [see Eq. (11)]. In this case, Eq. (9) shows that the overall temperature polarization coefficient is similar to the temperature polarization coefficient in the feed side, θ_f .



4. If the heat transfer in the feed membrane side is very large, the temperature at the feed side membrane surface and the temperature corresponding to the bulk phase are very similar. From Eq. (10), the feed temperature polarization coefficient, θ_f , approaches unity. In this case, the temperature polarization coefficient in the permeate side is important and is similar to the overall temperature polarization coefficient, θ .

Similarly to the temperature polarization coefficient given in Eq. (9), the vapor pressure polarization coefficient may be defined as:

$$\eta = \eta_f + \eta_p - 1 \quad (12)$$

where η_f , η_p are, respectively, the vapor pressure polarization coefficients in the feed and in the permeate and may be defined as in Eqs. (10) and (11).

$$\eta_f = \frac{P_v(x_f, T_f) - P_v(T_{bp})}{P_v(x_{bf}, T_{bf}) - P_v(T_{bp})} \quad (13)$$

$$\eta_p = \frac{P_v(x_{bf}, T_{bf}) - P_v(T_p)}{P_v(x_{bf}, T_{bf}) - P_v(T_{bp})} \quad (14)$$

where x_{bf} and x_f are the molar solute concentrations in the bulk feed and at the feed membrane surface, respectively.

The vapor pressure of distilled water can be determined from Antoine equation.^[2] For salt solutions, the effect of solute concentration on the partial vapor pressure should be taken into account.^[1,3] The following relation was given elsewhere.^[1]

$$P_v(x, T) = a(x, T)P_v^0(T) \quad (15)$$

in which $P_v^0(T)$ represents the vapor pressure of distilled water and $a(x, T)$ the water activity in the salt aqueous solution.

The methods used in the present study to determine the polarization coefficients are discussed in the following sections.

Velocity Extrapolation Method

The contribution of the boundary layers to the decrease of the thermal effects in DCMD has been studied extensively by Mengual and Peña,^[1] Velázquez and Mengual,^[5] and Khayet et al.^[6] The method proposed by those investigators is based on the fact that the thickness of the boundary layer decreases with the flow rate (i.e., with the circulation velocity). By performing measurements of the permeated flux at different circulation velocities and



extrapolating the data to an infinite velocity, the temperature polarization effect was estimated. This method is extended in this work to determine the vapor pressure polarization coefficients of the feed and permeate membrane sides as well as the overall one.

From previous research,^[1,5,6] the following relationship can be achieved.

$$\frac{1}{N} = A_0 + \frac{A_1}{v^\gamma} \quad (16)$$

where A_0 and A_1 are functions depending on the system parameters, v is the circulation velocity, and γ is a positive dimensionless number.

This equation was obtained from the study of heat transfer through thermal boundary layers and from the dependence of the Nusselt number, which is proportional to the heat transfer coefficient, on the Reynolds number, which is proportional to the circulation velocity, by means of Eq. (17):

$$h = a_0 v^\gamma \quad (17)$$

where a_0 is a fitting parameter.

According to Eq. (16), the MD flux increases with the circulation velocity as indicated by the experiments. The value of the MD flux, N_∞ , that would correspond to an infinite circulation velocity, in absence of polarization effects, may be obtained from the parameter A_0 ($A_0 = 1/N_\infty$). In this case, the coefficient η may be rewritten as:^[1]

$$\eta = \frac{N}{N_\infty} \quad (18)$$

It must be mentioned that for a given vapor pressure difference, Eq. (16) may be written as:

$$\frac{1}{B_b} = A'_0 + \frac{A'_1}{v^\gamma} \quad (19)$$

where A'_0 and A'_1 are functions depending on the system parameters. From the value of A'_0 , the net MD coefficient, B , may be obtained ($B = 1/A'_0$).

In this method, the existence of concentration polarization, which should affect the flux measurement in a similar way as the temperature polarization, is also considered when testing salt aqueous solutions.

To determine the overall vapor pressure polarization coefficient, η , the MD flux was measured at equal feed and permeate circulation velocity and this was increased simultaneously maintaining constant the mean bulk transmembrane temperature difference. For each experiment, the global MD coefficient was calculated and a plot of $(1/B_b)$ vs. $(1/v^\gamma)$ should yield an intercept of $(1/B)$, from which η may be obtained using Eq. (4).



To obtain the coefficients η_f and η_p , the same procedure was used but one of the circulation velocities was maintained constant at a given value, while the other circulation velocity was varied. For example, to determine the vapor pressure polarization coefficient in the permeate side, η_p , the measured MD flux at different feed circulation velocities, v_f , were fitted to Eq. (16), from which the MD flux corresponding to infinite feed circulation velocity, $N_{f\infty}$, can be determined. This corresponds to the theoretical absence of the polarization in the feed side. Finally, η_p may be evaluated using Eq. (18) for the given permeate circulation velocity.

Similarly, to determine the vapor pressure polarization coefficient in the feed side, η_f , the experiments carried out at different permeate circulation velocities, v_p , for a given value of v_f , permit to get a value of the MD flux in absence of polarization in the permeate side, $N_{p\infty}$. Then, Eq. (18) permits us to get η_f for the feed circulation velocities, v_f .

Semiempirical Method

In the MD published reports, several equations for the calculation of the temperatures of the feed and permeate at the membrane surfaces have been presented.^[3,8] In this study, Eq. (5) permits us to write the temperatures T_f and T_p as:

$$T_f = \frac{((\varepsilon k_g + (1 - \varepsilon)k_m)/(\delta))(T_{bp} + (h_f/h_p)T_{bf}) + h_f T_{bf} - N\lambda}{((\varepsilon k_g + (1 - \varepsilon)k_m)/(\delta)) + h_f(1 + (\varepsilon k_g + (1 - \varepsilon)k_m)/(\delta h_p))} \quad (20)$$

$$T_p = \frac{((\varepsilon k_g + (1 - \varepsilon)k_m)/(\delta))(T_{bf} + (h_p/h_f)T_{bp}) + h_p T_{bp} + N\lambda}{((\varepsilon k_g + (1 - \varepsilon)k_m)/(\delta)) + h_p(1 + (\varepsilon k_g + (1 - \varepsilon)k_m)/(\delta h_f))} \quad (21)$$

In Eqs. (20) and (21), the heat-transfer coefficients h_f and h_p can be determined assuming that the Nusselt number is given by the following heat transfer empirical correlations.

For the feed circulating in the lumen side of the membrane module under laminar flow regime:^[4]

$$Nu = \frac{h_f d_h}{k} = 1.86 \left(Re Pr \frac{d_h}{L} \right)^{1/3} \quad (22)$$

where Nu , Re , and Pr are the Nusselt, Reynolds, and Prandtl numbers, respectively; d_h is the equivalent diameter of the flow channel; k is the thermal conductivity, and L is the module length.



For transitional flow:^[9]

$$Nu = \frac{h_f d_h}{k} = 0.116 (Re^{2/3} - 125) Pr^{1/3} \left[1 + \left(\frac{d_h}{L} \right)^{2/3} \right] \quad (23)$$

For turbulent flow:^[2]

$$Nu = \frac{h_f d_h}{k} = 0.023 Re^{4/5} Pr^{0.4} \quad (24)$$

For the permeate circulating in the shell side of the membrane module, parallel and cross flow may occur simultaneously. In this case, the following correlation proposed in Kreith and Bohn^[10] was used:

$$Nu = \frac{h_p d_h}{k} = 0.206 (Re \cos \alpha)^{0.63} Pr^{0.36} \quad (25)$$

where α is the yaw angle, which varies between 0° , for pure cross-flow, and 90° , for pure parallel flow.^[10]

In addition, the concentration polarization coefficient, ξ , can be evaluated from the interfacial concentration given by the following equation:^[1,3]

$$\xi = \frac{C_f}{C_{bf}} = \exp(N/\rho K) \quad (26)$$

where C_{bf} and C_f are the solute concentration at the bulk feed solution and at the membrane surface, respectively; ρ is the liquid density, and K is the solute mass-transfer coefficient.

The method that is always used in MD investigations to determine the mass-transfer coefficient is to employ an analogy between heat and mass transfers. In this study, Eqs. (22) through (24) were used to estimate the coefficient, K , by substituting the Sherwood number (Kd_h/D_s) for the Nusselt number and the Schmidt number ($\mu/\rho D_s$) for the Prandtl number, with D_s being the diffusion coefficient of the solute and μ the bulk liquid viscosity.

Finally, from Eqs. (10) and (11), the temperature polarization coefficients, θ_f and θ_p , may be determined and Eqs. (13) and (14) permit the evaluation of the vapor pressure polarization coefficients, η_f and η_p . Consequently, the overall temperature polarization coefficient, θ , and the overall vapor pressure polarization coefficient, η , may be calculated from Eqs. (9) and (12), respectively.



RESULTS AND DISCUSSION

In this study, initial experiments were conducted to check the linear relationship between the MD flux and the bulk vapor pressure difference between the feed and permeate as indicated in Eqs. (1) through (4). In this case, distilled water was used as feed and the MD flux was measured at various bulk temperature differences between the feed and permeate, varying from 12.5°C to 40°C. Similarly, the tangential circulation velocity was varied from 0.2 m/s to 1 m/s, at equal feed and permeate circulation velocities. The mean temperature was fixed at 42.5°C. Figure 3 shows the obtained MD flux as a function of the transmembrane bulk vapor pressure difference. For each circulation velocity, the pairs of values $(N; \Delta P_{vb})$ were fitted to a linear function by using the least squares method. The correlation coefficients were higher than 0.99. Therefore, the linear agreement of the experimental data in Fig. 3 may be considered good in our system. The calculated global MD coefficient, B_b , was 103.9×10^{-9} s/m, 116.6×10^{-9} s/m, 125×10^{-9} s/m, and 132.8×10^{-9} s/m, for the tangential circulation velocities 0.2 m/s, 0.4 m/s, 0.6 m/s, and 1 m/s, respectively. As can be observed, the global MD coefficient increases with the circulation velocity. This result confirms the existence of the vapor pressure polarization, which has lesser importance at higher circulation velocity. This fact was observed earlier in DCMD systems and other MD configurations, such as sweeping gas membrane distillation (SGMD) and vacuum membrane distillation (VMD).^[3-5,7,11]

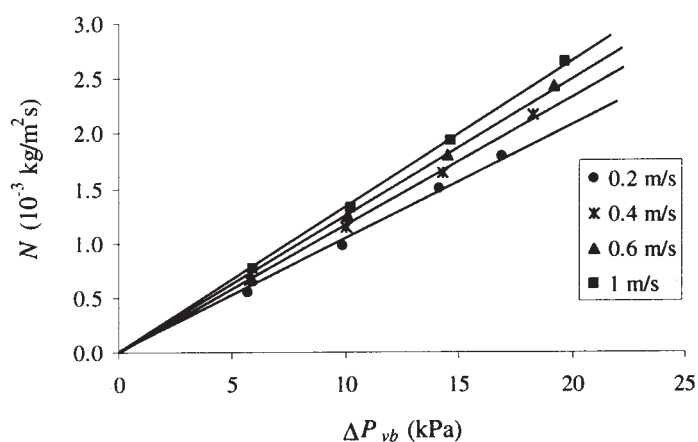


Figure 3. MD flux (N) as function of the transmembrane bulk vapor pressure at different liquid circulation velocities ($v_f = v_p$). The solid lines represent the linear fits of the experimental data according to Eq. (1).



The obtained B_b values were fitted to the circulation velocity ($v_f = v_p = v$) according to Eq. (19) by using a nonlinear χ^2 -minimization method. The correlation coefficient was 0.997, which confirms that the method used is adequate. The γ value was 0.42 and the calculated value of the net MD coefficient, B , from the extrapolation to infinite circulation velocity was 188.3×10^{-9} s/m. This value coincides with the one calculated using Eqs. (1) through (3) and a tortuosity factor of 1.13. In fact, for microfiltration membranes used in MD systems, a value of 2 for the pore tortuosity is frequently assumed to fit the theoretical data to the experimental ones.^[2,11-13] However, for tubular module constituted of polypropylene (PP) membranes of pore size 0.45 μm , Laganà et al.^[14] assumed a lower value of the tortuosity factor (i.e., 1.3) to determine the simulated flux in a DCMD process applied for concentration of dilute aqueous apple juice solutions. Lawson and Lloyd^[15] employed various PP flat-sheet membranes of different pore sizes in DCMD configuration with pore tortuosity values between 1.29 and 1.65. From the gas permeation experiments, Bandini et al.^[11] found a value of unity for the polytetrafluoroethylene (PTFE) membranes of pore size 0.2 μm . For the same membrane in our previous work, we found an almost similar value, 1.1.^[16]

From Eq. (4), the global vapor pressure polarization coefficient, η , may be calculated. The obtained η values were 55.2%, 61.9%, 66.4%, and 70.5%, for the velocities 0.2 m/s, 0.4 m/s, 0.6 m/s, and 1 m/s, respectively. This indicates that from 29.5% to 44.8% of the driving force (i.e., transmembrane vapor pressure) is dissipated in both the hot and the cold boundary layers. Martínez et al.^[4] found values between 40% and 60% when using PTFE membrane with a pore size 0.2 μm in a DCMD configuration. For pure water DCMD, the highest values of the temperature polarization coefficient reported in the literature fall within 40% for membranes with high permeability to 70% for membranes with low fluxes.^[2] However, Lawson and Lloyd^[15] obtained a value as high as 85%. In fact, for well-designed systems, the polarization coefficients approach unity and for systems having large boundary layer resistances (i.e., high concentration and temperature polarization) the polarization coefficients approach zero.

To diminish the polarization effect, it is important to know the contribution of each membrane side. For this reason, the second set of experiments consisted of the measurements of the MD flux at various feed and permeate circulation velocities under the same transmembrane bulk temperature difference and mean temperature. Sodium chloride solutions of electrical conductivities $4 \pm 1 \mu\text{S}/\text{cm}$ (distilled water), $78 \pm 1 \mu\text{S}/\text{cm}$ (≈ 1 molar), and $135 \pm 1 \mu\text{S}/\text{cm}$ (≈ 2 molar) were used as feed. The results are summarized in Table 1.

An examination of the table shows that in all cases, the dependence of the MD flux on the circulation velocity confirms the presence of the boundary layers in both the feed and permeate sides, as the MD flux increases with both



Table 1. MD flux ($\times 10^{-6}$ kg/m² s) measured at various circulation velocities and sodium chloride concentrations.

Feed v_f (m/s)	Permeate v_p (m/s)	4 μ S/cm, $T_{bf} = 48.5^\circ\text{C}$, $T_{bp} = 22^\circ\text{C}$	4 μ S/cm $T_{bf} = 62^\circ\text{C}$, $T_{bp} = 22^\circ\text{C}$	78 μ S/cm $T_{bf} = 62^\circ\text{C}$, $T_{bp} = 22^\circ\text{C}$	135 μ S/cm $T_{bf} = 62^\circ\text{C}$, $T_{bp} = 22^\circ\text{C}$
0.2	0.2	901.3	2033.9	1919.8	1802.9
0.4	0.4	1044.2	2289.6	2174.5	2034.7
0.6	0.6	1100.3	2441.5	2327.4	2209.4
0.8	0.8	1156	2529.9	2421.3	2266.5
1	1	1184.4	2585.6	2473.3	2335.2
∞	∞	1432.5	3318.3	3246.6	3145.8
		990.8	2214.8	2016.7	1882
		1101.5	2408.8	2256.6	2105.3
0.2		1128.1	2480.7	2360.4	2242.8
0.4		1168.1	2534.9	2437.8	2292
0.6	1	1184.4	2585.6	2473.3	2335.2
0.8		1200.6	2650	2514.3	2362.1
1		1277.8	2863.9	2774.4	2669.8
		1136.8	2467.2	2375.1	2201.9
		1158.9	2527.2	2415.9	2268.1
0.2		1170.8	2540.5	2451.2	2287.2
0.4		1178	2560.8	2472.2	2310.5
0.6		1184.4	2585.6	2473.3	2335.2
0.8		1306.4	2966.5	2870.2	2720.4
		936.4	2105.6	—	—
0.2		1077.1	2341.1	—	—
0.4		1100.3	2441.1	—	—
0.6	0.6	1153.2	2500.9	—	—
0.8		1170.8	2539.9	—	—
1		1191.3	2583.5	—	—
∞		1249.7	2758.2	—	—
		1015.7	2324.2	—	—
		1070.2	2393.4	—	—
0.2		1100.3	2441.1	—	—
0.4		1118.4	2459.7	—	—
0.6	0.8	1128.1	2480.7	—	—
0.8		1268.2	2868	—	—



the feed and permeate circulation velocities. It is worth noticing that the effect of the permeate circulation velocity on the MD flux is lower than the effect of the feed circulation velocity. This may be due to the asymmetric vapor pressure polarization. In fact, the values of the MD flux were fitted to the corresponding varied circulation velocity (v_f , v_p or both v_f and v_p) by the least squares procedure using Eq. (16). The obtained correlation coefficients were higher than 0.97 and the dependence of the MD flux on the variable circulation velocity was found to be adequate. The values of the MD fluxes, $N_{f\infty}$, $N_{p\infty}$, and N_∞ , obtained respectively from the extrapolation to infinite feed circulation velocity at fixed permeate circulation velocity, infinite permeate circulation velocity at constant feed circulation velocity, and infinite feed and permeate circulation velocities, are also presented in Table 1.

Figure 4 shows the calculated global vapor pressure polarization coefficient, η , using Eq. (18), as a function of the circulation velocity, that is, at equal feed and permeate circulation velocities ($v_f = v_p = v$). As observed previously, the global vapor pressure polarization coefficient increases with the simultaneous increases of the circulation velocities of feed and permeate. When using distilled water as feed, the vapor pressure polarization effect is lower at low bulk feed temperature. This result was assured previously for the temperature polarization effect in DCMD.^[4,5] In addition, η decreases with an increase of the feed solute concentration, and this may be attributable to the increase of the concentration polarization. This result is discussed later.

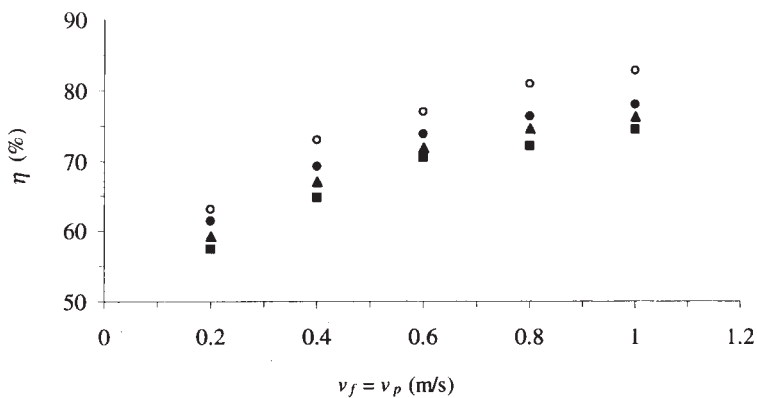


Figure 4. Calculated global vapor pressure polarization coefficient, η , as a function of the circulation velocity ($v_f = v_p$) for different bulk feed temperature (T_{bf}), different bulk feed electrical conductivities (χ), and permeate bulk temperature (T_{bp}) of 22°C: (○) for $\chi = 4 \mu\text{S}/\text{cm}$ and $T_{bf} = 48.5^\circ\text{C}$; (●) for $\chi = 4 \mu\text{S}/\text{cm}$ and $T_{bf} = 62^\circ\text{C}$; (▲) for $\chi = 78 \mu\text{S}/\text{cm}$; and (■) for $\chi = 135 \mu\text{S}/\text{cm}$ and $T_{bf} = 62^\circ\text{C}$.



As it was indicated in the theoretical section, the MD flux, $N_{f\infty}$, was determined from the extrapolation of the feed circulation velocity to infinite, using Eq. (16), and the experimental MD flux obtained at fixed permeate velocity (i.e., 0.6 and 1 m/s). This corresponds to the theoretical absence of vapor pressure polarization in the feed side. In this case, by using Eq. (18), the η_p was determined for the circulation velocities 0.6 and 1 m/s. Similarly, the η_f values were evaluated in the same way for 0.6 and 1 m/s from the MD flux, $N_{p\infty}$, obtained from the extrapolation to infinite permeate circulation velocity. Finally, from Eq. (12), the global vapor pressure polarization coefficient was evaluated for each circulation velocity (0.6 and 1 m/s). The results are given in Table 2.

As can be observed in Table 2, the vapor pressure polarization coefficients, η_f , η_p , and η , increase with the circulation velocity; and for the same circulation velocity, those coefficients decrease as the solute feed concentration increases. In all cases, the vapor pressure polarization in the permeate side, η_p , is higher than the vapor pressure polarization in the feed side, η_f , and η is lower than η_f and η_p . It must be mentioned that the values of η calculated from Eq. (18) were almost similar to the ones calculated from Eq. (12), with the weighted standard deviation within 1.5%.

In the other hand, for each experimental run, the temperature polarization coefficients, θ_f , θ_p , and θ , the concentration polarization coefficient, ζ , as well as the vapor pressure polarization coefficients, η_f , η_p , and η were determined as explained previously using the semiempirical method. The obtained results of the same experimental data as in Table 2 are presented in Table 3. As an example, Figure 5 shows the obtained values of the vapor pressure polarization coefficients (η_f , η_p , and η) vs. the circulation velocity ($v_f = v_p = v$)

Table 2. Feed, permeate, and global vapor pressure polarization coefficients obtained from the velocity extrapolation method.

$v_f = v_p$ (m/s)	T_{bf} (°C)	χ ($\mu\text{S}/\text{cm}$)	η_f	η_p	η^a	η^b
0.6	48.5	4	86.76	88.04	74.80	76.81
	62	4	85.11	88.5	73.61	73.58
1	48.5	4	90.66	92.69	83.35	82.62
	62	4	87.16	90.28	77.44	77.92
	62	78	86.17	89.15	75.32	76.18
	62	135	85.84	87.47	73.31	74.23

^aCalculated from Eq. (12) using the obtained values of η_f and η_p .

^bCalculated from Eq. (18) using the experimental data presented in the first five rows of Table 1 ($v_f = v_p = v$).



Table 3. Feed, permeate, and global temperature polarization coefficients and vapor pressure polarization coefficients obtained from the semiempirical method.

$v_f = v_p$ (m/s)	T_{bf} (°C)	χ ($\mu\text{S}/\text{cm}$)	θ_f	θ_p	θ	η_f	η_p	η
0.6	48.5	4	91.50	87.26	78.76	86.01	93.24	79.25
	62	4	93.97	84.62	78.59	88.04	93.91	81.95
1	48.5	4	96.52	89.95	86.47	94.11	94.77	88.88
	62	4	96.92	88.08	85.00	93.76	95.45	89.22
	62	78	95.09	88.45	83.55	90.01	95.46	85.47
	62	135	94.22	88.83	83.04	88.05	95.44	83.49

when distilled water was used as feed, the bulk permeate temperature, T_{bp} , was 22°C, and the bulk feed temperature, T_{bf} , was 62°C.

In all cases, the values of the temperature polarization coefficient in the feed side, θ_f , are higher than the values of the temperature polarization coefficient in the permeate side, θ_p . However, as observed in Table 2, the vapor pressure polarization coefficient in the feed side, η_f , was lower than the vapor pressure polarization coefficient in the permeate side, η_p . This may be due to the exponential variation of the vapor pressure with temperature. In addition, θ_f values are higher than η_f values within 3 and 7%. This may be attributed to the

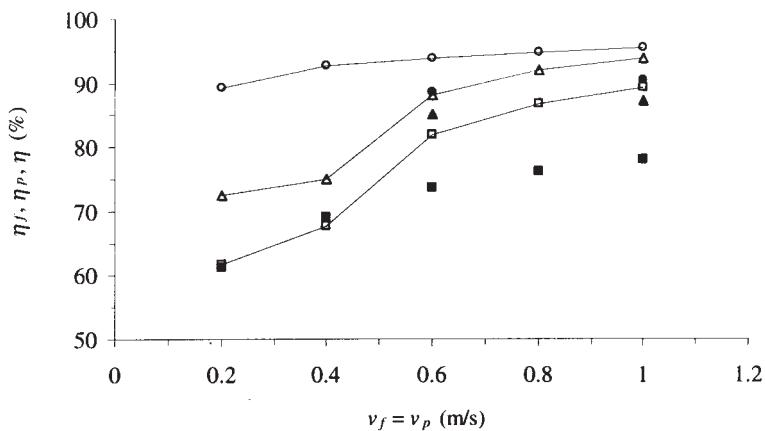


Figure 5. Calculated vapor pressure polarization coefficients, η_f , η_p , and η , as a function of the circulation velocity ($v_f = v_p$) using the velocity extrapolation method [(●) for η_p , (▲) for η_f , (■) for η] and the semiempirical method [(○) for η_p , (Δ) for η_f , (□) for η].



effect of the concentration polarization coefficient, which occurred in the feed side. In fact, for the circulation velocity of 1 m/s, the estimated concentration at the membrane feed side was 4.0% (for the feed solution 78 $\mu\text{S}/\text{cm}$) and 4.4% (for the feed solution 135 $\mu\text{S}/\text{cm}$) higher than that of the bulk concentration. This corresponds to a decrease of the vapor pressure of only 0.1% and 0.2%, respectively. Consequently, the concentration polarization implies a negligible reduction in the MD flux. It was reported^[3] that the effect of sodium chloride on the MD flux is mainly due to the vapor pressure reduction and to the raised viscosity, which causes a decrease of turbulence; and the concentration polarization has an insignificant influence.

Furthermore, as reported in our previous article,^[5] the global temperature polarization coefficient, θ , decreases slightly with the increase of the feed temperature. As can be observed in Table 3, the temperature polarization coefficient in the feed side increases when the feed side temperature increases; however, the temperature polarization coefficient in the permeate side decreases. In all cases, the θ values are lower than the η values within 0.5% and 4.7%. In previous research,^[4] it was noticed that the vapor pressure polarization coefficient differ less than 0.6% of the temperature polarization coefficient when distilled water was used as feed, and the difference is higher when the NaCl concentration is increased. In Table 3, for the same circulation velocity (i.e., 1 m/s), it can be observed that the temperature polarization coefficient in the feed side, θ_f , becomes closer to the vapor pressure polarization coefficient in the feed side, η_f , as the salt concentration decreases.

From the results of the polarization coefficients reported in Tables 2 and 3, for the circulation velocities 0.6 m/s and 1 m/s, the global vapor pressure polarization coefficients calculated using the semiempirical method were higher than the ones obtained from the velocity extrapolation method. However, as presented in Fig. 5, at lower circulation velocity (i.e., $v < 0.6 \text{ m/s}$), the η values obtained from the two methods were almost similar. This may be due to the selected empirical correlations used to calculate the heat-transfer coefficients in the lumen side and the shell side of the membrane module. In fact, those empirical correlations were developed for nonporous heat exchangers and in MD systems, heat transfer is coupled with mass transfer. A critical review of the most frequently used empirical heat transfer correlations was presented recently^[17] and special care must be taken into account when those correlations are used in MD processes.

CONCLUSION

Theoretical and experimental study of DCMD in a shell-and-tube capillary membrane module was presented. The temperature polarization

coefficients and the vapor pressure polarization coefficients in each membrane side as well as the concentration polarization coefficient in the feed side were defined and evaluated. Two methods, the velocity extrapolation method and the semiempirical method, were used to determine the polarization coefficients in the feed and permeate side of the membrane. Distilled water and NaCl aqueous solutions were used. The effect of the feed circulation velocity, the permeate circulation velocity and the feed temperature on the MD flux has been evaluated. The following conclusions were made.

1. An asymmetric temperature polarization and vapor pressure polarization through the composite system "hot boundary layer-membrane-cold boundary layer" exist.
2. The concentration polarization was insignificant and the temperature polarization in the feed side was higher than the temperature polarization in the permeate side.
3. The vapor pressure polarization coefficient in the permeate side was higher than the vapor pressure polarization in the feed side.
4. The global temperature polarization coefficient was slightly lower than the global vapor pressure polarization coefficient.
5. Because the driving force in an MD separation process is the transmembrane vapor pressure, the vapor pressure polarization coefficient should be used instead of using both the concentration and temperature polarization coefficients.
6. The global vapor pressure polarization coefficients determined using the extrapolation velocity method were lower than the corresponding coefficients determined using the semiempirical method, especially at high circulation velocities. This may be attributed to the selected empirical correlations developed for nonporous heat exchangers and used in the semiempirical method to calculate the heat-transfer coefficients.

SYMBOLS

a = water activity.

a_0 = fitting parameter in Eq. (17).

A_0 = adjustment parameter in Eq. (16).

A_1 = adjustment parameter in Eq. (16).

A_0' = adjustment parameter in Eq. (19).

A_1' = adjustment parameter in Eq. (19).

B = net MD coefficient ($\text{kg}/\text{m}^2 \cdot \text{s} \cdot \text{Pa}$).



B_b = global MD coefficient ($\text{kg}/\text{m}^2 \cdot \text{s} \cdot \text{Pa}$).
 C = solute concentration (mol/m^3).
 d_h = hydraulic diameter (m).
 D = diffusion coefficient (m^2/s).
 h = heat-transfer coefficient ($\text{W}/\text{m}^2 \cdot \text{K}$).
 H = overall heat-transfer coefficient ($\text{W}/\text{m}^2 \cdot \text{K}$).
 k = thermal conductivity ($\text{W}/\text{m} \cdot \text{K}$).
 K = solute mass-transfer coefficient (m/s).
 L = channel length (m).
 M = molecular mass of water (kg/mol).
 N = MD water flux ($\text{kg}/\text{m}^2 \cdot \text{s}$).
 Nu = Nusselt number.
 P = pressure (Pa).
 Pr = Prandtl number.
 r = pore size (m).
 R = gas constant ($\text{J}/\text{mol} \cdot \text{K}$).
 Re = Reynolds number.
 T = temperature (K).
 v = liquid circulation velocity (m/s).
 x = liquid mole fraction.

Greek Letters

α = yaw angle of the membrane module ($^\circ$).
 δ = membrane thickness (m).
 ε = fractional void volume.
 γ = positive dimensionless number.
 η = vapor pressure polarization coefficient.
 λ = heat of vaporization of water (J/kg).
 μ = viscosity ($\text{kg}/\text{m} \cdot \text{s}$).
 θ = temperature polarization.
 ρ = density (kg/m^3).
 τ = pore tortuosity.

Subscripts

a = air.
 b = bulk.
 d = molecular diffusion.
 f = feed.



g = gas.
 k = Knudsen diffusion.
 m = membrane matrix.
 p = permeate.
 s = solute.
 v = water vapor.
 ∞ = infinite.

Superscripts

0 = distilled water.

ACKNOWLEDGMENT

Economical support from the CICYT is acknowledged.

REFERENCES

1. Mengual, J.I.; Peña, L. Membrane distillation. *Colloid & Surface Sci.* **1997**, *1*, 17–29.
2. Schofield, R.W.A.; Fane, A.G.; Fell, C.J.D. Heat and mass transfer in membrane distillation. *J. Membr. Sci.* **1987**, *33*, 299–313.
3. Schofield, R.W.A.; Fane, A.G.; Fell, C.J.D.; Macoun, R. Factors affecting flux in membrane distillation. *Desalination* **1990**, *77*, 279–294.
4. Martínez-Díez, L.; Vázquez-González, M.I. Temperature and concentration polarization in membrane distillation of aqueous salt solutions. *J. Membr. Sci.* **1999**, *156*, 265–273.
5. Velázquez, A.; Mengual, J.I. Temperature polarization coefficients in membrane distillation. *Ind. Eng. Chem. Res.* **1995**, *34* (2), 585–590.
6. Khayet, M.; Godino, M.P.; Mengual, J.I. Modeling transport mechanism through a porous partition. *J. Non-Equilibrium Thermodyn.* **2001**, *26*, 1–14.
7. Khayet, M.; Godino, M.P.; Mengual, J.I. Theory and experiments on sweeping gas membrane distillation. *J. Membr. Sci.* **2000**, *165* (2), 261–272.
8. Gryta, M.; Tomaszewska, M. Heat transport in the membrane distillation process. *J. Membr. Sci.* **1998**, *144*, 211–222.



9. Gröber, H.; Erk, S. Trasmisión del calor en convección forzada y régimen turbulento. In *Transmisión de Calor*, 1st Spanish Ed.; Selecciones Científicas: Madrid, 1967; 256–288.
10. Kreith, F.; Bohn, M.S. Forced convection over exterior surfaces. In *Principle of Heat Transfer*, 5th Ed.; PWS Publish. Comp.: Boston, 1997; 445–497.
11. Bandini, S.; Saavedra, A.; Sarti, G.C. Vacuum membrane distillation: experiments and modeling. *AIChE J.* **1997**, *43*, 398–408.
12. Gostoli, C. Thermal effects in osmotic distillation. *J. Membr. Sci.* **1999**, *163*, 75–91.
13. Banat, F.A.; Al-Rub, F.A.; Jumah, R.; Al-Shannag, M. Modeling of desalination using tubular direct contact membrane distillation modules. *Sep. Sci. & Tech.* **1999**, *34* (11), 2191–2206.
14. Laganà, F.; Barbieri, G.; Drioli, E. Direct contact membrane distillation: modelling and concentration experiments. *J. Membr. Sci.* **2000**, *166*, 1–11.
15. Lawson, K.W.; Lloyd, D.R. Membrane distillation. II. Direct contact MD. *J. Membr. Sci.* **1996**, *120*, 123–133.
16. Khayet, M.; Godino, P.; Mengual, J.I. Nature of flow on sweeping gas membrane distillation. *J. Membr. Sci.* **2000**, *170*, 243–255.
17. Mengual, J.I.; Khayet, M.; Godino, M.P. A critical review of the empirical heat transfer correlations used in membrane distillation, 12th Annual Meeting of the North American Membrane Society, Lexington, Kentucky, USA, May, 15–20, 2001; Bhattacharyya, D., Butterfield, D.A., Carlson, L., Eds.; University of Kentucky: Lexington, 2001; 195. *Membrane Transport Models II-7*.

Received October 2002

Revised June 2003



Request Permission or Order Reprints Instantly!

Interested in copying and sharing this article? In most cases, U.S. Copyright Law requires that you get permission from the article's rightsholder before using copyrighted content.

All information and materials found in this article, including but not limited to text, trademarks, patents, logos, graphics and images (the "Materials"), are the copyrighted works and other forms of intellectual property of Marcel Dekker, Inc., or its licensors. All rights not expressly granted are reserved.

Get permission to lawfully reproduce and distribute the Materials or order reprints quickly and painlessly. Simply click on the "Request Permission/Order Reprints" link below and follow the instructions. Visit the [U.S. Copyright Office](#) for information on Fair Use limitations of U.S. copyright law. Please refer to The Association of American Publishers' (AAP) website for guidelines on [Fair Use in the Classroom](#).

The Materials are for your personal use only and cannot be reformatted, reposted, resold or distributed by electronic means or otherwise without permission from Marcel Dekker, Inc. Marcel Dekker, Inc. grants you the limited right to display the Materials only on your personal computer or personal wireless device, and to copy and download single copies of such Materials provided that any copyright, trademark or other notice appearing on such Materials is also retained by, displayed, copied or downloaded as part of the Materials and is not removed or obscured, and provided you do not edit, modify, alter or enhance the Materials. Please refer to our [Website User Agreement](#) for more details.

Request Permission/Order Reprints

Reprints of this article can also be ordered at

<http://www.dekker.com/servlet/product/DOI/101081SS120027405>